

An innovative dry-lab test rig for mechanical-hydraulic power take-off of wave energy conversion system

Mohd Afifi Jusoh, Zulkifli Mohd Yusop, Aliashim Albani, Muhamad Zalani Daud,
Mohd Zamri Ibrahim

Renewable Energy and Power Research Interest Group (REPRIG), Eastern Corridor Renewable Energy Special Interest Group,
Faculty of Ocean Engineering Technology and Informatics, Universiti Malaysia Terengganu, Kuala Nerus, Malaysia

Article Info

Article history:

Received Jul 6, 2023

Revised Oct 23, 2023

Accepted Nov 7, 2023

Keywords:

Experiment test rig

Mechanical-hydraulic

Power take-off

Renewable energy

Wave energy conversion system

ABSTRACT

A dry-lab test rig is a powerful means to reduce costs in the design process of a wave energy conversion system (WECs). A dry-lab test rig technique allows the use of real components inside a simulation of a mathematical model. This paper presents the development of an innovative dry-lab test rig for the mechanical-hydraulic power take-off (MHPTO) unit of WECs. The development of a dry-lab test rig of MHPTO involves several processes, such as three-dimension (3D) modelling, component purchasing, structure fabrication, component installation, and operational testing. The developed dry-lab test rig consists of two main parts, such as the simulated wave emulator plant and the real MHPTO unit plant. The simulated wave emulator plant was developed in this test rig to replicate the interaction motion between the ocean wave motion and the wave absorber device. The developed dry-lab test rig was tested using five different irregular wave input conditions to ensure it could perform under the five different wave input conditions. The overall results demonstrate that the developed dry-lab test rig was successfully performed in all sea states. From the results, the profile of electrical power produced by the real MHPTO unit can be clearly obtained in each sea state.

This is an open access article under the [CC BY-SA](#) license.



Corresponding Author:

Mohd Zamri Ibrahim

Renewable Energy and Power Research Interest Group (REPRIG), Eastern Corridor Renewable Energy Special Interest Group, Faculty of Ocean Engineering Technology and Informatics, Universiti Malaysia Terengganu
Kuala Nerus, Terengganu, Malaysia

Email: zam@umt.edu.my

1. INTRODUCTION

Over the world, various technologies of wave energy conversion system (WECs) have been developed to harvest energy from ocean resources and transform it into usable electrical power. Recent studies have discovered over a thousand WECs that have been granted patents worldwide, particularly in Europe, North America, and Japan [1]-[3]. Existing WECs consist of a number of major components, including the wave absorber device, the power take-off unit, the electrical power converter, and the control system unit [4]-[8].

The power take-off (PTO) unit is among the most significant components of WECs since it directly corresponds to the quantity of wave energy turned into useful electricity. Additionally, the size and weight of the PTO unit have a direct effect on the dynamic design of WECs. According to [5], [6], [9]-[11], several PTO unit designs have been created, developed, and experimentally tested for different kinds of wave absorber systems during the last few decades. On the basis of their fundamental operating principles, the different PTO

ideas may be categorised as a direct electrical drive (linear generator), direct mechanical drive, hydro-turbine, air-turbine and mechanical-hydraulic [9]. Mechanical-hydraulic power take-off (MHPTO) unit stands out as one of the most robust and efficient PTO units for WECs [12]. The MHPTO unit excels in a number of respects, including its high efficiency, broad controllability, and compatibility with the low frequency and high power density of ocean waves [13]-[15]. The MHPTO unit may be constructed with standard hydraulic parts [16].

Nowadays, the optimisation of the MHPTO unit during the design process of WECs is a crucial issue. An accurate simulation model of the MHPTO unit is essential to reproduce the dynamics behaviour and understand the performance of the actual MHPTO unit. Also, the developed MHPTO mathematical model can be used for power quality assessment and control systems development. Experimental validation is essential for producing a precise mathematical model of the MHPTO unit. It is preferable to validate the experiment in a safe and controlled environment since interventions in remote locations might be highly costly and unfeasible owing to weather conditions. A dry-lab testing scheme is considered as an alternative way to bridge the gap between the laboratory and the real application environment. In the wave energy sector, many dry-lab test rigs have been utilised to evaluate several kinds of PTO units [17]-[23]. However, only a few dry-lab test rigs based on the MHPTO unit have been developed [17]. In addition, to the best of our knowledge, there is no dry-lab test rig based on the considered wave absorber device, and MHPTO unit concepts have been developed worldwide. Therefore, the present work adds a new contribution to the development of an innovative dry-lab test rig for MHPTO testing. The rest of the paper is organised as follows: section 2 describes the details of the considered WECs concept and a dry-lab test rig. Section 3 presents the results and discussion from the dry-lab test rig testing. Finally, section 4 concludes the paper.

2. METHOD

2.1. Wave energy conversion system

Figure 1(a) presents a complete view of proposed WECs design for the shoreline area in Malaysia [24]. This WECs was designed with a capacity of 10 kW. In this concept, the WECs is integrated with the fixed platform, as illustrated in Figure 1(b). The multiple rotation-based wave absorber devices are attached to the fixed platform facing toward the dominant ocean wave direction. The MHPTO transforms the energy from the wave motions captured by wave absorber devices into useful electrical power. The MHPTO and the control system units of the WECs are separately installed on top of the fixed platform. The wave absorber devices are connected to the MHPTO unit via hydraulic actuators. Then, hydraulic hoses connect the hydraulic actuators to the other parts of the MHPTO unit. In addition, the wave absorber devices are equipped with an automated floater level control that allows them to function at any sea level.

There are several advantages of the future WECs concept presented in Figure 1. The overall energy conversion efficiency using this WECs is high since the MHPTO unit is considered in this concept. This WECs concept also has less marine environment impacts since most of the WECs equipments are located above the water surface. This WECs also required less development cost compared to offshore-based WECs. The WECs design is also uncomplicated; thus, it can be constructed by local experts using common construction equipment. This WECs concept also is easy to access for regular maintenance work. Finally, the WECs device in this concept is able to operate at any ocean tide level, particularly during the monsoon season.

Recently, the development of the proposed WECs concept presented in Figure 1 is still at an earlier stage. Several investigations are required to be carried out, particularly on the MHPTO unit, to optimise the overall WECs operation in a real sea state. For this reason, the present work was conducted to initially analyse the behaviour and performance of the MHPTO unit in order to ensure that optimal electrical power can be generated from the MHPTO unit. Figure 2(a) illustrates the simplified WECs concept based on the future WECs concept presented in Figure 1. A simplified concept was designed with a capacity of 100 W. In this concept, a single MHPTO unit is connected to a single wave absorber device through a single hydraulic actuator. The MHPTO unit concept based on the constant pressure concept is considered in this WECs model, as illustrated in Figure 2(b). In this MHPTO unit concept, single-rod double-acting hydraulic cylinders are used as hydraulic actuators to maximise mechanical energy absorption during bi-directional wave absorber devices pitch motion [25]. The hydraulic actuator module is connected to the rectification module, which consists of the four non-return check valves (CV_1 , CV_2 , CV_3 & CV_4) through hydraulic hoses. The rectification module is then connected to the generation module, which includes a fixed displacement hydraulic motor (HM) coupled with the permanent magnet synchronous generator (G). The fluid energy storage module comprises two bladder-type

hydraulic accumulators, namely a high-pressure accumulator (HPA) and a low-pressure accumulator (LPA), placed between the rectification module and generation module. Additionally, the pressure relief valve (RV) is installed on the high-pressure line to avoid the over-pressurised event in the MHPTO unit.

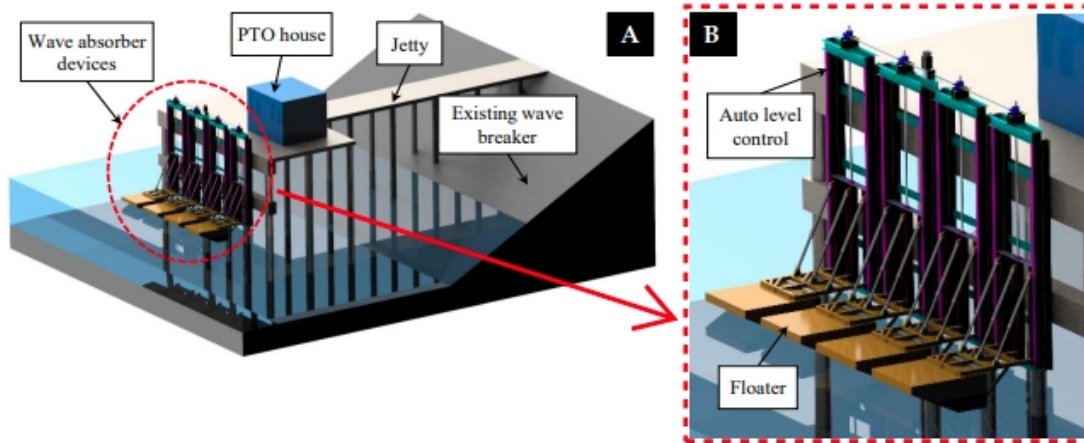


Figure 1. Conceptual design of future WECs for the shoreline area in Malaysia: (a) a complete view and (b) enlarged image of wave absorber device

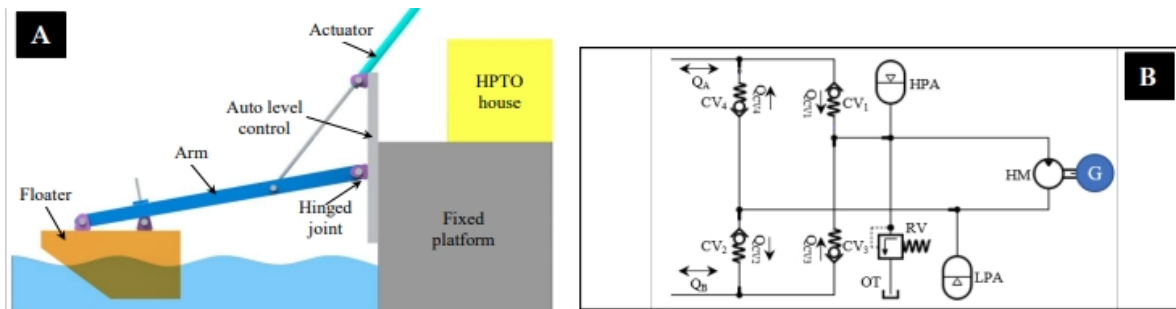


Figure 2. A simplified designed of WECs: (a) Wave absorber device and (b) MHPTO unit

2.2. Dry-lab test rig design

A physical model of the WECs is required to experimentally evaluate the accuracy of the MHPTO unit model. Thus, a dry-lab test rig based on the WECs concept was developed in the present study. Developing a dry-lab test rig of WECs involves several processes, such as 3D modelling, components purchasing, structure fabrication, components installation and operational testing. Initially, the design process of a dry-lab test rig was carried out using Solid Edge software in order to generate an accurate design test rig. Several important factors were considered during the design process, such as the overall cost, material selection, transportation, et cetera. Figure 3(a) illustrates a complete 3D model design of the dry-lab test rig. The view of the actual dry-lab test rig of WECs is depicted in Figure 3(b). Figure 4 illustrates a simplified architecture of a developed dry-lab test rig. Based on the figure, the developed dry-lab test rig consists of two main parts: the simulated wave emulator plant and the real MHPTO unit plant. The details of the simulated wave emulator plant and the real MHPTO unit plant are described in sections 2.2.1 and 2.2.2.

2.2.1. Simulated wave emulator plant

The simulated wave emulator plant was developed in this test rig to replicate the interaction motion between the wave absorber device and the ocean wave motion. The replicated relative pitch motion of the wave absorber device is utilised to drive a real MHPTO unit. The wave emulator plant consists of a floater’s arm, electric linear actuator, servo motor drive, data acquisition (DAQ) board, DAQ interface and computer with

MATLAB/Simulink. In this plant, the electric linear actuator was placed between the floater's arm and the fixed platform using pillow bearings, as illustrated in Figure 3. The rest components of the wave emulator unit were placed in the control system panel.

As seen in Figure 4, the generalised wave excitation force profile created offline based on wave parameters is the input of the wave emulator plant. The generated wave excitation force and the hydraulic actuator force, F_{MHPTO} that is measured through the force sensor are fed into the hydrodynamic wave absorber device model in order to evaluate a desired relative linear displacement of a hydraulic actuator, $x_{HA,d}$ in real-time. Meanwhile, the real-time linear displacement of the hydraulic actuator, $x_{HA,act}$ that is measured through an infrared linear displacement sensor is compared with the desired linear displacement input. The comparison output from the controller (Δi) is then used by the servo drive to control the linear actuator speed in order to ensure the actual displacement of the hydraulic actuator tracks the desired one. Thus, the relative pitch motion of the floater due to the wave motions, which drive the hydraulic actuator of the MHPTO unit in the real environment can be duplicated. This indicates that a dry-lab test rig enables inexpensive "dry tests" on the MHPTO unit of WECs. Thus, the dry-lab test rig capability makes the test rig a valuable instrument for evaluating the electrical power generated by the WECs, Figure 5 illustrates the simplified diagram of the wave emulator control system.

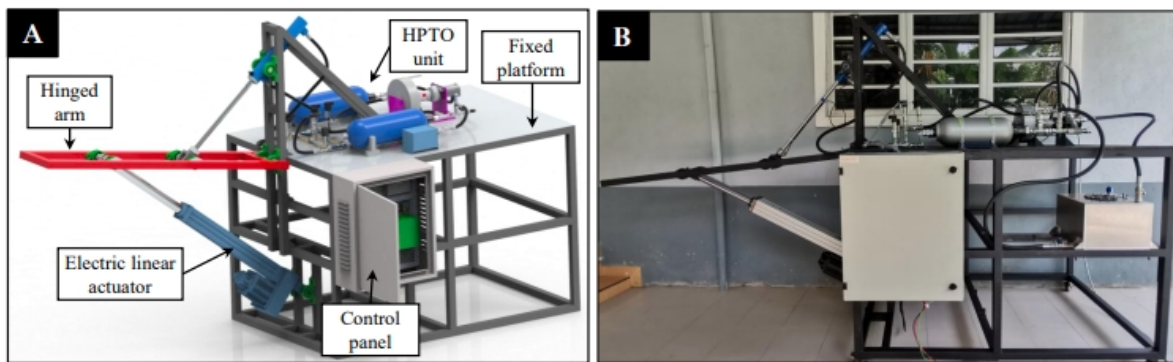


Figure 3. Images of a dry-lab test rig of WECs: (a) a 3D design model in solid Edge software and (b) the actual setup of test rig of WECs

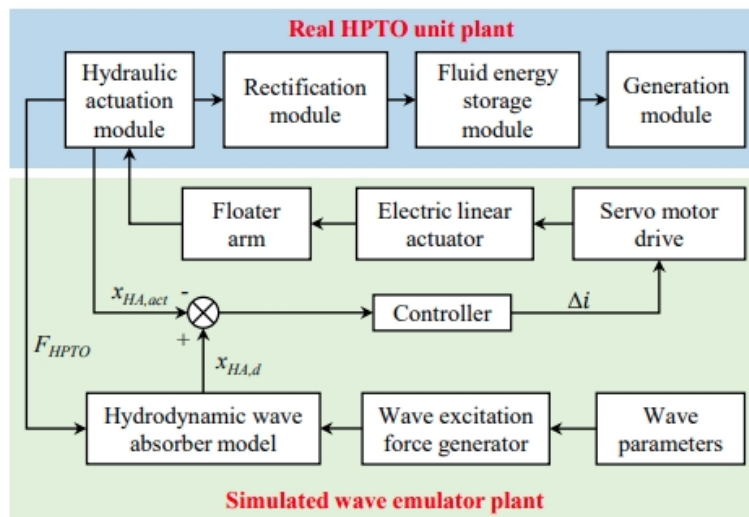


Figure 4. A simplified architecture of a developed dry-lab test rig

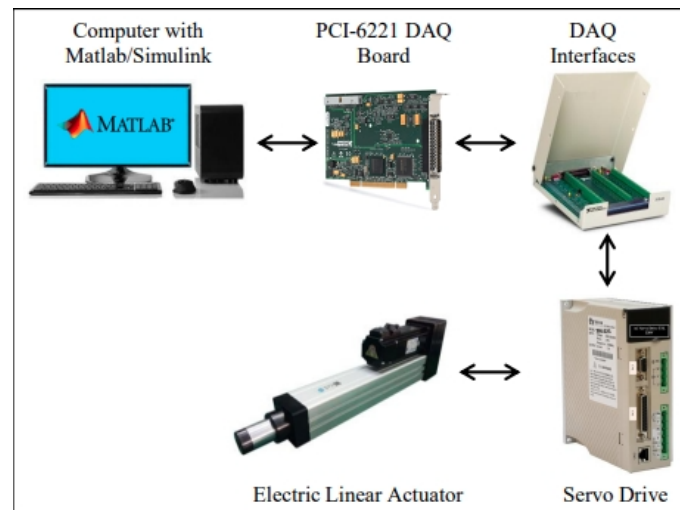


Figure 5. Simplified diagram of wave emulator control

2.2.2. Real MHPTO unit plant

Figure 6 shows the enlarged image of a real MHPTO unit plant in a dry-lab test rig. The barrel and rod sides of the hydraulic actuation module were attached to the fixed platform and floater's arm using a pillow bearing. The rest MHPTO unit components were placed on top of the fixed platform. The specifications of each component in the real MHPTO unit plant are summarised in Table 1. Besides that, several sensors were installed to measure important data in the real MHPTO unit plant. Pressure transducers were utilised to measure the pressures in the chambers of the hydraulic actuator. The force resisted by the hydraulic actuator is measured by a force sensor installed at the end piston rod. The infrared linear displacement sensor was employed at the hydraulic actuator barrel to measure hydraulic actuator displacement. The speed of the generator is measured by the speed sensor placed between the hydraulic motor and the generator. The power produced by the generator is measured by a power meter. The simplified diagram of the data logger system for the sensor in the real MHPTO unit plant is depicted in Figure 7.

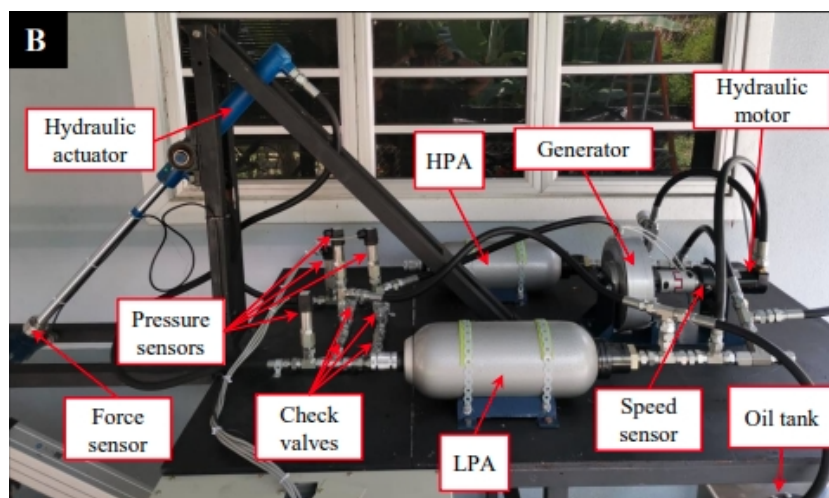


Figure 6. Enlarged image of real MHPTO unit plant

Table 1. Technical specifications of components in real the MHPTO unit plant

Module	Specifications	
Actuation	Stroke length: 0.3 m Rod diameter: 0.025 m	Piston diameter: 0.035 m
Rectification	Discharge coefficient: 0.95	Opening area : 0.003 m
Fluid energy storage	HPA precharge pressure: 40.0 bar HPA volume capacity: 2.0 L	LPA precharge pressure: 5.0 bar LPA volume capacity: 2.0 L
Generation	Generator rated power: 100 W Generator rated speed: 200 rpm Generator rated torque: 6.0 Nm	Generator damping coefficient: 0.03 Nm/rpm Hydraulic motor displacement: 8.0 cc/rev

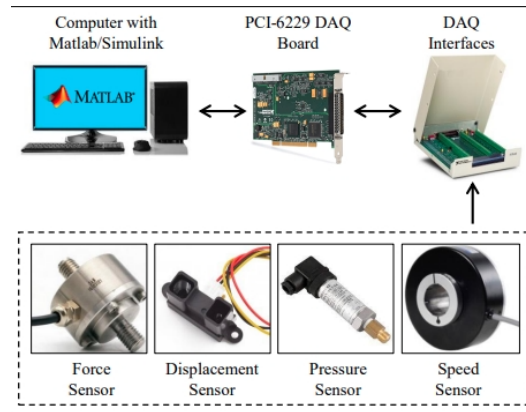


Figure 7. Esimplified diagram of data logger system for real the MHPTO unit plant

3. RESULTS AND DISCUSSION

The developed dry-lab test rig was tested using five different irregular wave input data to ensure it can able to perform in the five different wave input conditions. Sea state A (SSA) is intended to test the developed dry-lab test rig in nominal sea state. The significant wave height (H_s) and peak wave period (T_p) in SSA were fixed to 0.8 m and 4.5 s. Sea states B and C (SSB and SSC) are intended to test the developed dry-lab test rig in different H_s conditions. For SSB and SSC, the H_s was adjusted to 0.6 m and 1.0 m, which ± 0.2 m of the nominal H_s , but T_p was retained at its nominal value. Meanwhile, Sea states D and E (SSD and SSE) are intended to test the developed dry-lab test rig in different T_p conditions. For SSD and SSE, H_s was kept at its nominal value whereas T_p was adjusted to 2.5 s and 6.5 s which ± 2.0 s of the nominal T_p . In Addition, the developed dry-lab test rig was tested for a 60 s period for each case. The testing results of the developed dry-lab test rig are presented in sections 3.1 and 3.2.

3.1. Operational behaviour of MHPTO unit in different sea states

Figure 8 presents the operating behaviour of the specified MHPTO unit components for SSA. The reactions of the hydraulic actuator piston to the irregular wave input in SSA are shown in Figure 8(a). The result in Figure 8(a) illustrates that the hydraulic actuator piston's displacement was significantly smaller than the wave elevation. According to the data, the hydraulic actuator piston's average displacement was 15% of the wave elevation. Besides that, the result in Figure 8(a) demonstrates a minor delay between the hydraulic actuator piston's displacement and the wave height. Figure 8(b) illustrates the MHPTO unit force profile applied to the wave absorber device. During movements up and down, the MHPTO forces applied to the wave absorber device averaged 3.71 kN and 1.66 kN, respectively. The unbalanced force of the MHPTO unit applied to the wave absorber device was due to the asymmetrical piston area [16]. A larger piston area side generated more force than one with a smaller piston area. Figure 8(c) depicts the pressure profile of the HPA (P_{HPA}). Based on the data, the maximum pressure of HPA was 42.2 bar, a 5.5% increase over its pre-charge pressure setting. Figure 8(d) shows the hydraulic motor speed (ω_{HM}) profile. The hydraulic motor speed was consistently below 200 rpm, as seen by the graph.

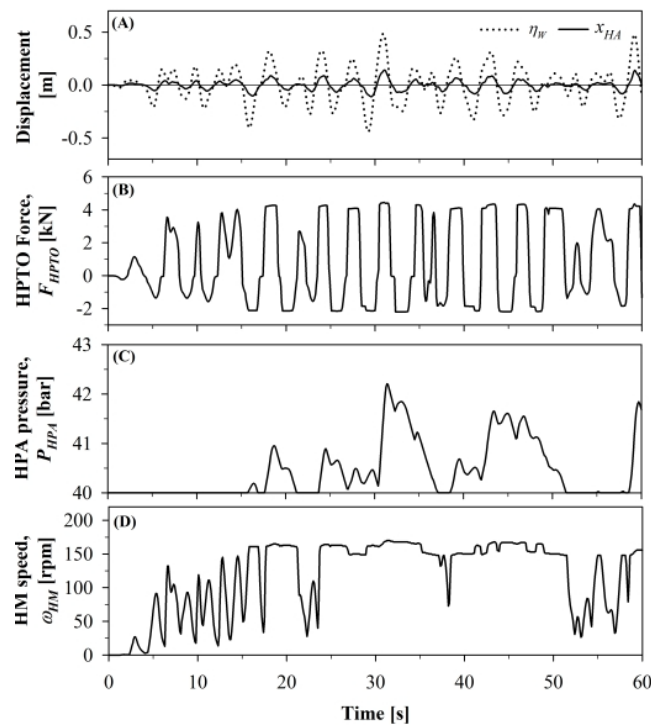


Figure 8. Operational behaviour of selected MHPTO unit components in SSA: (a) Hydraulic actuator displacement, (b) Hydraulic actuator force, (c) HPA pressure, and (d) Hydraulic motor speed

The operating behaviours of the MHPTO unit in each sea condition are compared in Table 2. According to the data shown in the table, H_s and T_p affect the overall MHPTO unit performance. Based on the table, the average displacement of the hydraulic actuator piston varied in response to changes in both H_s and T_p , increasing or decreasing accordingly. The average hydraulic actuator piston displacement in sea states SSB and SSD was reduced by 29.2% and 23.8% (during upward motion) and 24.9% and 16.7% (during downward motion) compared to the piston's displacement in the SSA. Meanwhile, the average hydraulic actuator piston displacement in the SSC and SSE were increased by 24.7% and 17.4% (during upward motion) and 23.8% and 17.6% (during downward motion), respectively.

Table 2. Operational behaviour of the non-optimal MHPTO unit for different sea states

Descriptions	Sea state				
	A	B	C	D	E
Actuation module					
$P_{HA,ave}$ [bar]	A 25.70	21.17	30.03	21.57	26.54
	B 23.88	18.14	28.17	20.17	24.03
F_{MHPTO} [kN]	↑ 3.708	3.097	4.274	3.228	3.795
	↓ 1.657	1.293	2.202	1.405	1.633
$x_{HA,ave}$ [m]	↑ 0.038	0.027	0.048	0.029	0.045
	↓ 0.040	0.030	0.049	0.033	0.047
Energy storage module					
$P_{HPA,max}$ [bar]	42.22	40.79	45.53	41.09	42.82
Generation module					
$P_{HM,ave}$ [bar]	40.61	31.63	47.19	35.07	40.29
$\omega_{HM,ave}$ [rpm]	152.8	114.7	181.4	128.6	152.8

The increase and decrease of average displacement of the hydraulic actuator piston relatively increased and decreased the pressure and speed of the hydraulic motor, as presented in Table 2. As can be seen, the average speed of the hydraulic motor in SSB and SSD decreased by 24.9% and 15.8% of its speed in SSA,

while 23.8% and 14.7% were increased in SSC and SSE. Overall, the power output of the MHPTO unit is below its rated capacity throughout all sea states.

3.2. Electrical power produced by the MHPTO unit in various sea states

Figure 9 presents the results of electrical power produced by the MHPTO unit in SSA to SSE. The red dashed line represents the rated power of the MHPTO unit. Overall, the results from Figures 9(a) to 9(e) show that the electrical power produced by the MHPTO unit in SSA to SSE was significantly lower than the rated power of the MHPTO unit, particularly in low H_s and T_p sea states (SSB and SSD). In the nominal H_s and T_p sea state (SSA), the MHPTO unit produced electrical power up to the average of 61.39 W, which is 38.61% lower than the rated power, as depicted in Figure 9(a). In lower and higher H_s sea states (SSB and SSC), the average generated power from the MHPTO unit was only up to 39.09 W and 84.87 W, as shown in Figures 9(b) and 9(c). Meanwhile, in lower and higher T_p sea states, the average generated power from the MHPTO unit were only up to 46.07 W and 67.37 W, as illustrated in Figures 9(d) and 9(e), respectively.

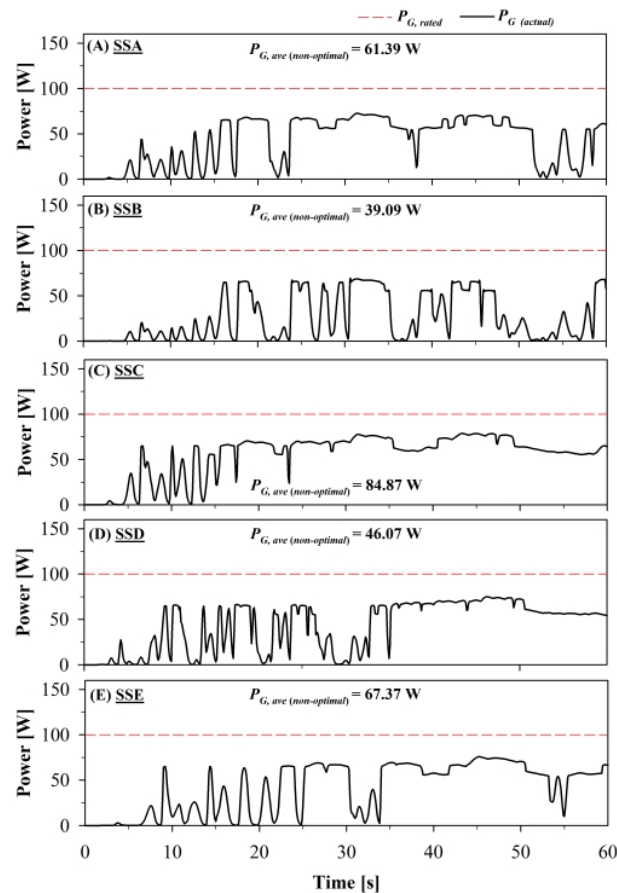


Figure 9. Comparison of electrical power produced by MHPTO unit in various sea states: (a) SSA, (b) SSB, (c) SSC, (d) SSD, and (e) SSE

4. CONCLUSION

In this paper, an innovative dry-lab test rig for the MHPTO unit of WECs is presented. The development of a dry-lab test rig of WECs involves several processes, such as 3D modelling, structure fabrication, components installation and operational testing. The developed dry-lab test rig consists of two main parts: the simulated wave emulator plant and the real MHPTO unit plant. The simulated wave emulator plant was developed in this test rig to replicate the interaction motion between the ocean wave motion and the wave absorber device. The replicated relative pitch motion of the wave absorber device is utilised to drive a real MHPTO unit. To demonstrate the performance of the dry-lab test rig under different operating conditions, several tests were

carried out using five different irregular wave input data. The overall results demonstrate that the developed dry-lab test rig was successfully performed in all sea states. From the results, the profile of electrical power produced by the real MHPTO unit can be clearly obtained in each sea state. The dry-lab test rig was developed based on the dry-lab condition. Thus, the experimental validation of the developed dry-lab test rig with the wave tank-based dry-lab test rig is required to validate its effectiveness in real hydrodynamic conditions. Therefore, the experimental validation of the developed dry-lab test rig should be explored in the future.

ACKNOWLEDGEMENTS

The work reported here has been supported by the Ministry of Higher Education (MOHE) and Universiti Malaysia Terengganu (UMT). The authors would like to thank to the MOHE for the research funding under the Fundamental Research Grant Scheme (FRGS/1/2019/TK07/UMT/01/1).




REFERENCES

- [1] D. Jovicic, "Series LC DC circuit breaker," *High Voltage*, vol. 4, no. 2, pp. 130–137, Jun. 2019, doi: 10.1049/hve.2019.0003.
- [2] P. Pareek and H. D. Nguyen, "Probabilistic robust small-signal stability framework using gaussian process learning," *Electric Power Systems Research*, vol. 188, p. 106545, Nov. 2020, doi: 10.1016/j.epsr.2020.106545.
- [3] S. Leonelli and N. Tempini, *Data Journeys in the Sciences*. Cham: Springer International Publishing, 2020, doi: 10.1007/978-3-030-37177-7.
- [4] G. Nguyen et al., "Machine learning and deep learning frameworks and libraries for large-scale data mining: a survey," *Artificial Intelligence Review*, vol. 52, no. 1, pp. 77–124, Jun. 2019, doi: 10.1007/s10462-018-09679-z.
- [5] R. Vinayakumar, M. Alazab, K. P. Soman, P. Poornachandran, A. Al-Nemrat, and S. Venkatraman, "Deep learning approach for intelligent intrusion detection system," *IEEE Access*, vol. 7, no. 9 Special Issue 3, pp. 41525–41550, Aug. 2019, doi: 10.1109/ACCESS.2019.2895334.
- [6] K. Sivaraman, R. M. V. Krishnan, B. Sundarraj, and S. Sri Gowthem, "Network failure detection and diagnosis by analyzing syslog and SNS data: Applying big data analysis to network operations," *International Journal of Innovative Technology and Exploring Engineering*, vol. 8, no. 9 Special Issue 3, pp. 883–887, Aug. 2019, doi: 10.35940/ijitee.I3187.0789S319.
- [7] A. D. Dwivedi, G. Srivastava, S. Dhar, and R. Singh, "A decentralized privacy-preserving healthcare blockchain for IoT," *Sensors (Switzerland)*, vol. 19, no. 2, p. 326, Jan. 2019, doi: 10.3390/s19020326.
- [8] F. Al-Turjman, H. Zahmatkesh, and L. Mostarda, "Quantifying uncertainty in internet of medical things and big-data services using intelligence and deep learning," *IEEE Access*, vol. 7, no. 1, pp. 115749–115759, Mar. 2019, doi: 10.1109/ACCESS.2019.2931637.
- [9] S. Kumar and M. Singh, "Big data analytics for healthcare industry: Impact, applications, and tools," *Big Data Mining and Analytics*, vol. 2, no. 1, pp. 48–57, Mar. 2019, doi: 10.26599/BDMA.2018.9020031.
- [10] L. M. Ang, K. P. Seng, G. K. Ijamaru, and A. M. Zungeru, "Deployment of IoV for smart cities: applications, architecture, and challenges," *IEEE Access*, vol. 7, pp. 6473–6492, Dec. 2019, doi: 10.1109/ACCESS.2018.2887076.
- [11] B. P. L. Lau et al., "A survey of data fusion in smart city applications," *Information Fusion*, vol. 52, no. 1, pp. 357–374, Dec. 2019, doi: 10.1016/j.inffus.2019.05.004.
- [12] Y. Wu et al., "Large scale incremental learning," in *Proceedings of the IEEE Computer Society Conference on Computer Vision and Pattern Recognition*, Jun. 2019, vol. 2019-June, no. 4, pp. 374–382, doi: 10.1109/CVPR.2019.00046.
- [13] A. Mosavi, S. Shamshirband, E. Salwana, K. wing Chau, and J. H. M. Tah, "Prediction of multi-inputs bubble column reactor using a novel hybrid model of computational fluid dynamics and machine learning," *Engineering Applications of Computational Fluid Mechanics*, vol. 13, no. 1, pp. 482–492, Jan. 2019, doi: 10.1080/19942060.2019.1613448.
- [14] V. Palanisamy and R. Thirunavukarasu, "Implications of big data analytics in developing healthcare frameworks – A review," *Journal of King Saud University - Computer and Information Sciences*, vol. 31, no. 4, pp. 415–425, Oct. 2019, doi: 10.1016/j.jksuci.2017.12.007.
- [15] J. Sadowski, "When data is capital: Datafication, accumulation, and extraction," *Big Data and Society*, vol. 6, no. 1, p. 205395171882054, Jan. 2019, doi: 10.1177/2053951718820549.
- [16] J. R. Saura, B. R. Herreraez, and A. Reyes-Menendez, "Comparing a traditional approach for financial brand communication analysis with a big data analytics technique," *IEEE Access*, vol. 7, pp. 37100–37108, 2019, doi: 10.1109/ACCESS.2019.2905301.
- [17] D. Nallaperuma et al., "Online incremental machine learning platform for big data-driven smart traffic management," *IEEE Transactions on Intelligent Transportation Systems*, vol. 20, no. 12, pp. 4679–4690, Dec. 2019, doi: 10.1109/TITS.2019.2924883.
- [18] S. Schulz, M. Becker, M. R. Groseclose, S. Schadt, and C. Hopf, "Advanced MALDI mass spectrometry imaging in pharmaceutical research and drug development," *Current Opinion in Biotechnology*, vol. 55, pp. 51–59, Feb. 2019, doi: 10.1016/j.copbio.2018.08.003.
- [19] C. Shang and F. You, "Data analytics and machine learning for smart process manufacturing: Recent advances and perspectives in the big data era," *Engineering*, vol. 5, no. 6, pp. 1010–1016, Dec. 2019, doi: 10.1016/j.eng.2019.01.019.
- [20] Y. Yu, M. Li, L. Liu, Y. Li, and J. Wang, "Clinical big data and deep learning: Applications, challenges, and future outlooks," *Big Data Mining and Analytics*, vol. 2, no. 4, pp. 288–305, Dec. 2019, doi: 10.26599/BDMA.2019.9020007.
- [21] M. Huang, W. Liu, T. Wang, H. Song, X. Li, and A. Liu, "A queuing delay utilization scheme for on-path service aggregation in services-oriented computing networks," *IEEE Access*, vol. 7, pp. 23816–23833, 2019, doi: 10.1109/ACCESS.2019.2899402.
- [22] G. Xu, Y. Shi, X. Sun, and W. Shen, "Internet of things in marine environment monitoring: A review," *Sensors (Switzerland)*, vol. 19, no. 7, p. 1711, Apr. 2019, doi: 10.3390/s19071711.
- [23] M. Aqib, R. Mehmood, A. Alzahrani, I. Katib, A. Albeshri, and S. M. Altowajiri, "Smarter traffic prediction using big data, in-memory computing, deep learning and gpus," *Sensors (Switzerland)*, vol. 19, no. 9, p. 2206, May 2019, doi: 10.3390/s19092206.




- [24] N. Stylos and J. Zwiendelaar, "Big data as a game changer: How does it shape business intelligence within a tourism and hospitality industry context?," in *Big Data and Innovation in Tourism, Travel, and Hospitality: Managerial Approaches, Techniques, and Applications*, Singapore: Springer Singapore, 2019, pp. 163–181.
- [25] Q. Song, H. Ge, J. Caverlee, and X. Hu, "Tensor completion algorithms in big data analytics," *ACM Transactions on Knowledge Discovery from Data*, vol. 13, no. 1, pp. 1–48, Feb. 2019, doi: 10.1145/3278607.

BIOGRAPHIES OF AUTHORS






Mohd Afifi Jusoh    received his first degree in Electrical Engineering from University Teknologi MARA (UiTM), Shah Alam, Malaysia in 2013. He then obtained his M.Sc. degree in Electronics and Instrumentation from Universiti Malaysia Terengganu, Malaysia in 2018. Currently, he is pursuing his Ph.D. in Electricity and Energy at Universiti Malaysia Terengganu, Malaysia. His research interests include battery energy storage applications, distributed generation and renewable energy. He has published several papers in reputable conferences and journals in the field of renewable energy. He is a member of the Board Of Engineers Malaysia. He can be contacted at email: mohd.afifi.jusoh@gmail.com.






Zulkifli Mohd Yusop    received his BEng (Electronic) major in Control and Instrumentation from Universiti Teknologi Malaysia, Johor, Malaysia at the Faculty of Electrical in 2010. In 2017 he completed his PhD in Mechanical Engineering, core in Applied Mechanics and Control at the same university. Currently, he is a Senior Lecturer at the Faculty of Ocean Engineering Technology and Informatics, Universiti Malaysia Terengganu. His research interest is in robotics, smart energy management system and renewable energy. He can be contacted at email: zulkifli.yusop@umt.edu.my.






Aliashim Albani    received his PhD, MSc and BTech in Environmental Technology from Universiti Malaysia Terengganu. Currently, he is a Senior Lecturer at the Faculty of Ocean Engineering Technology and Informatics, Universiti Malaysia Terengganu. His research interest is Renewable Energy and Environmental Technology. He can be contacted at email: a.albani@umt.edu.my.



Muhamad Zalani Daud    received his BEng (Electrical and Electronic) and MEng from Ritsumeikan University in Kyoto, Japan and the School of Electrical, Computer and Telecommunications Engineering, University of Wollongong, NSW, Australia in 2003 and 2010, respectively. In April 2014 he completed his PhD in the Department of Electrical, Electronic & Systems Engineering, at Universiti Kebangsaan Malaysia in Bangi Malaysia. Currently, he is an Associate Professor at the Faculty of Ocean Engineering Technology and Informatics, Universiti Malaysia Terengganu. His research interest is in battery energy storage applications, distributed generation and renewable energy. He can be contacted at email: zalani@umt.edu.my.



Mohd Zamri Ibrahim    received his first Degree in Mechanical Engineering from the University of Sunderland, UK in 1995. In 1997, he graduated from Warwick University, UK with a Master's Degree in Advanced Mechanical Engineering. In the year 2007, he completed his Ph.D. in Renewable Hydrogen Energy Production Systems at the National University of Malaysia, (UKM) Malaysia. Currently, he is a Professor at the Faculty of Ocean Engineering Technology and Informatics, Universiti Malaysia Terengganu. His recent work focused especially on renewable energy in the Renewable energy system and renewable energy Resources. It includes research interests in Renewable Energy System technology design and techno-economics studies such as wind, solar, wave, and ocean current energy. His research interests also concentrate on the fields of hydrogen fuel, energy sources forecasting, and clean technology system. He can be contacted at email: zam@umt.edu.my.